Landslides (2016) 13:293–303
DOI 10.1007/s10346-015-0569-2
Received: 13 September 2014
Accepted: 18 February 2015
Published online: 13 March 2015

Dian-Qing Li · Te Xiao · Zi-Jun Cao · Chuang-Bing Zhou · Li-Min Zhang

Enhancement of random finite element method in reliability analysis and risk assessment of soil slopes using Subset Simulation

Abstract Random finite element method (RFEM) provides a rigorous tool to incorporate spatial variability of soil properties into reliability analysis and risk assessment of slope stability. However, it suffers from a common criticism of requiring extensive computational efforts and a lack of efficiency, particularly at small probability levels (e.g., slope failure probability P_f<0.001). To address this problem, this study integrates RFEM with an advanced Monte Carlo Simulation (MCS) method called "Subset Simulation (SS)" to develop an efficient RFEM (i.e., SS-based RFEM) for reliability analysis and risk assessment of soil slopes. The proposed SS-based RFEM expresses the overall risk of slope failure as a weighed aggregation of slope failure risk at different probability levels and quantifies the relative contributions of slope failure risk at different probability levels to the overall risk of slope failure. Equations are derived for integrating SS with RFEM to evaluate the probability (P_f) and risk (R) of slope failure. These equations are illustrated using a soil slope example. It is shown that the P_f and R are evaluated properly using the proposed approach. Compared with the original RFEM with direct MCS, the SS-based RFEM improves, significantly, the computational efficiency of evaluating P_f and R. This enhances the applications of RFEM in the reliability analysis and risk assessment of slope stability. With the aid of improved computational efficiency, a sensitivity study is also performed to explore effects of vertical spatial variability of soil properties on R. It is found that the vertical spatial variability affects the slope failure risk significantly.

Keywords Slope stability · Random finite element method · Subset Simulation · Reliability analysis · Risk assessment

Introduction

Slope stability analysis aims to evaluate the resistance of a natural or human-made slope to the failure by sliding along any slip surface, and to assess the safety margin of the slope against the sliding. The safety margin of slope stability is conventionally quantified by the factor of safety (FS), which is defined by comparing restoring to driving forces and/or moments, and can be calculated using various deterministic slope stability analysis methods, such as limit equilibrium methods (LEMs) (e.g., Duncan and Wright 2005) and finite element methods (FEMs) (e.g., Griffiths and Lane 1999). Although these deterministic slope stability analysis methods are widely adopted in slope engineering practice, they cannot, explicitly, account for the various geotechnical-related uncertainties (such as spatial variability in soil properties, uncertainties in loads, and calculation model uncertainty) and provide no information on the variability of safety margin of slope stability. In contrast, probabilistic slope stability analysis approaches provide a rational vehicle to, explicitly, incorporate various geotechnical-related uncertainties into slope engineering designs and quantify the safety margin of slope stability probabilistically by probability of failure (P_f) or reliability index (β) of slope stability.

In the past few decades, several probabilistic analysis approaches have been developed to evaluate the P_f or β of slope stability in geotechnical reliability community, such as the first order second moment method (e.g., Christian et al. 1994; Hassan and Wolff 1999), first order reliability method (e.g., Low et al. 1998; Cho 2013), and direct Monte Carlo Simulation (MCS) method (e.g., El-Ramly et al. 2002; Li et al. 2011; Zhang et al. 2011; Li et al. 2013, 2014; Tang et al. 2015) and its advanced variants (e.g., Ching et al. 2009; Wang et al. 2011). Although these efforts significantly facilitate the understanding and application of probability-based approaches in slope engineering, practicing engineers are reluctant to adopt them in slope engineering practice (e.g., El-Ramly et al. 2002). This dilemma can be attributed to, at least, two reasons, as observed by Griffiths and Fenton (2004) and Griffiths et al. (2009): (1) the majority of probabilistic slope stability analysis methods in previous studies make use of traditional slope stability analysis techniques, i.e., LEMs, which need to assume the shape and location of slope failure surfaces prior to the calculation and may fail to locate the most critical failure mechanism in highly variable soils; and (2) only the spatial variability of soil strength parameters along the critical slip surface identified by LEMs can be taken into account when using LEMs in the probabilistic analysis of slope stability.

To address the abovementioned problems, Griffiths and Fenton (2004) proposed a rigorous probabilistic analysis method called "random finite element method (RFEM)" for reliability analysis of slope stability. RFEM consists of three major components: random field theory (Vanmarcke 2010) to model inherent spatial variability of soil properties, FEM to assess the safety margin of slope stability, and MCS for uncertainty propagation and calculation of P_f. Griffiths et al. (2009) made use of RFEM to investigate the influences of spatial variability of soil strength parameters on slope stability. Huang et al. (2010) used RFEM to evaluate the system reliability of slope stability and pointed out that RFEM provides a general way to assess the system reliability of slopes. Then, Huang et al. (2013) combined RFEM with limit analysis and extended its application to risk assessment of slope failure. These studies have demonstrated the great potential of RFEM in reliability analysis and risk assessment of soil slopes. However, RFEM still suffers from a common criticism of requiring extensive computational efforts (e.g., Ji and Low 2012) and a lack of efficiency at small probability levels (e.g., P_f<0.001) because a large number of finite element analyses shall be performed in MCS to ensure the desired accuracy of the estimated P_f. Such a disadvantage becomes more profound when RFEM is applied to assess slope failure risk R, in which the average consequence ($\overline{C}$) of slope failure is also needed besides P_f (e.g., Huang et al. 2013) and the accurate estimation of $\overline{C}$ necessitates a large number of failure samples during MCS. This subsequently calls for an efficient RFEM

to evaluate P_f at small probability levels and to generate a large number of failure samples for estimating $\overline{C}$.

This paper proposes an efficient RFEM for reliability analysis and risk assessment of soil slopes, in which RFEM is enhanced by an advanced MCS called "Subset Simulation (SS)" to improve its computational efficiency of evaluating P_f and generating failure samples at small probability levels. The paper starts with a brief review of the original framework of RFEM, followed by development of the SS-based RFEM for reliability analysis and risk assessment of soil slopes. Then, the proposed approach is illustrated through a soil slope example. Finally, a sensitivity study is performed to explore effects of spatial variability on slope failure risk using the illustrative example.

Reliability analysis and risk assessment of slope stability using RFEM

Random field modeling of inherent spatial variability of soil properties in RFEM

RFEM provides a powerful and rigorous tool to incorporate inherent spatial variability of soil properties into slope stability analysis (e.g., Griffiths and Fenton 2004; Griffiths et al. 2009; Huang et al. 2010; Le 2014). It employs the random field theory (Vanmarcke 2010) to model the inherent spatial variability of soil properties, by which the soil property X (e.g., undrained shear strength S_u) in different elements of the finite element mesh adopted in slope stability analysis is represented by a series of spatially correlated random variables (i.e., a random field). For example, a two-dimensional (2-D) stationary lognormal random field $\boldsymbol{H}(X)$ can be used to model the inherent spatial variability of X in a statistically homogenous soil layer, where X in each element is represented by a lognormal random variable with a mean μ_X and standard deviation σ_X. Then, $\boldsymbol{H}(X)$ can be simulated using several random field generation techniques, such as the covariance matrix decomposition method (e.g., Wang et al. 2011; Wang and Cao 2013; Cao and Wang 2014), local average subdivision method (e.g., Fenton and Vanmarcke 1990), and Karhunen-Loève expansion method (e.g., Phoon et al. 2002; Cho 2010; Huang et al. 2013; Jiang et al. 2014). Consider, for example, using the covariance matrix decomposition method to simulate $\boldsymbol{H}(X)$ in this study, by which $\boldsymbol{H}(X)$ can be written as:

$$\boldsymbol{H}(X) = \exp(\mu_N \boldsymbol{l} + \sigma_N \boldsymbol{L}\boldsymbol{\xi}) \tag{1}$$

where $\mu_N = \ln\mu_X - \sigma_N^2/2$ and $\sigma_N = \sqrt{\ln\left[1 + (\sigma_X/\mu_X)^2\right]}$ are the mean and standard deviation of $\ln(X)$, respectively; $\boldsymbol{l}$=a vector with components that are all equal to unity; $\boldsymbol{\xi}=[\xi_1, \xi_2, \ldots, \xi_{Nz}]^T$=a standard Gaussian vector with N_z independent components; $\boldsymbol{L}$=a N_z-by-N_z lower-triangular matrix obtained from Cholesky decomposition of the correlation matrix $\boldsymbol{\rho}$ satisfying $\boldsymbol{\rho}=[\rho]=\boldsymbol{L}\boldsymbol{L}^T$ (e.g., Fenton and Griffiths 2008). ρ is the correlation coefficient between the values of $\ln(X)$ at different locations, and it is calculated from a prescribed spatial correlation function, e.g., a 2-D single exponential correlation function $\rho=\exp(-2|d_h|/\delta_h - 2|d_v|/\delta_v)$, where δ_h and δ_v are horizontal and vertical scale of fluctuation of $\ln(X)$, respectively, and d_h and d_v are horizontal and vertical distances between two different locations, respectively.

Finite element analysis of slope stability

As indicated by Eq. (1), $\boldsymbol{H}(X)$ is comprised of N_z spatially correlated random variables (i.e., X for different elements), each of which corresponds to one element of the finite element mesh adopted in finite element analysis of slope stability. For each realization of $\boldsymbol{H}(X)$, the N_z spatially correlated X random variables are simulated at the mid-point of the N_z elements of the finite element mesh in this study, and represent the value of X in each element. The simulated X values are used as inputs to perform the finite element analysis of slope stability and to calculate the FS of slope stability. In RFEM, the shear strength reduction technique (SSRT) (Matsui and San 1992; Griffiths and Lane 1999) is usually applied to calculate the FS, in which the slope failure is defined by the occurrence of non-convergence of solution in finite element analysis.

Calculation of slope failure probability and risk using direct MCS

After the uncertainty model (e.g., the random field model of soil properties) of uncertain parameters $\underline{\boldsymbol{X}}=[X_1, X_2, \ldots, X_{Np}]$ involved in slope stability analysis and deterministic finite element analysis modeling are set up, RFEM calculates the probability (P_f) and risk (R) of slope failure using direct MCS. Consider, for example, a direct MCS run with N_T realizations of $\underline{\boldsymbol{X}}$. For each realization of $\underline{\boldsymbol{X}}$, its corresponding FS is calculated using the SSRT. This leads to N_T values of FS. Then, P_f is calculated as:

$$P_f = \frac{1}{N_T}\sum_{i=1}^{N_T} I(FS_i < fs) \tag{2}$$

where fs=a threshold value for judging the slope failure, and it is usually taken as 1, corresponding to the failure criterion $FS<1$; $I(\cdot)$ is an indicator function of the occurrence of slope failure. For the i-th realization of $\underline{\boldsymbol{X}}$, $I(\cdot)$ is taken as the value of 1 when its corresponding FS_i is less than fs, i.e., $FS_i<fs$ occurs; otherwise, it is equal to 0. In addition, the coefficient of variation (COV_{P_f}) of P_f given by Eq. (2) can be estimated as (Ang and Tang 2007):

$$\mathrm{COV}_{P_f} = \sqrt{\frac{1-P_f}{P_f N_T}} \tag{3}$$

Then, the risk R of slope failure is conventionally calculated as:

$$R = P_f C \tag{4}$$

where C=consequence of slope failure. Equation (4) works well for a slope with a single failure mode (Huang et al. 2013). However, for a slope problem, there might exist multiple failure modes due to the spatial variability or stratification of geotechnical materials (e.g., Chowdhury and Xu 1995; Huang et al. 2010; Wang et al. 2011; Zhang et al. 2011; Li et al. 2013; Jiang et al. 2015). To account for the contributions of different failure modes to the overall risk of slope failure, Huang et al. (2013) extends Eq. (4) to a more general form:

$$R = \sum_{i=1}^{N_f} P_i C_i = P_f \overline{C} \tag{5}$$

where $P_i=1/N_T$ and C_i are the probability and consequence of the failure mode corresponding to the i-th failure sample during MCS,

respectively; $\overline{C}=\sum_{i=1}^{N_f} C_i/N_f$=the average consequence of different failure modes, in which N_f=the number of failure samples generated during MCS. As pointed out by Huang et al. (2013), the consequence of slope failure depends on the sliding mass volume, which can, therefore, be taken as an "equivalent" quantity to quantify the consequence of slope failure in slope risk assessment. Then, the average consequence $\overline{C}$ is estimated as the average of the sliding mass volume for different failure modes. For this purpose, the consequence C_i (i.e., the sliding mass volume) for the i-th failure sample generated during MCS needs to be estimated. This can be achieved by the K-means clustering method (KMCM) (Huang et al. 2013). KMCM is a popular and simple classification approach, and it aims to partition a set of observations into K clusters, in which each observation belongs to the cluster with the nearest mean value. For RFEM, node displacements obtained from the finite element analysis of slope stability are taken as observations in KMCM, and the element nodes of the finite element mesh are then classified into two clusters (i.e., K=2), including sliding and stable masses, based on node displacements. Let D_l and D_t denote the mean values of node displacements in sliding and stable masses, respectively. The element nodes whose displacements are closer to D_l than D_t are classified into sliding mass; otherwise, they belong to stable mass. Note that determining D_l and D_t is a key step in applying KMCM to identify stable and sliding masses, and this usually requires an iterative procedure, which can be referred to Huang et al. (2013) for more details. After stable and sliding masses are determined, the critical slip surface is taken as the boundary between them. Using the critical slip surface identified by KMCM, the sliding mass volume can be estimated if the slope failure occurs, and it is used in Eq. (5) to assess the slope failure risk.

Although direct MCS is a conceptually simple and robust method, it suffers from a lack of efficiency and resolution at small probability levels (e.g., P_f<0.001), which are of great interest in design practice. To improve the computational efficiency, RFEM is enhanced with Subset Simulation (SS) (Au and Beck 2001; Au and Wang 2014) in the next section.

Subset Simulation-based RFEM for slope reliability analysis and risk assessment

SS-based RFEM for reliability analysis of slope stability

SS stems from the idea that a small failure probability can be expressed as a product of larger conditional failure probabilities for some intermediate failure events, thereby converting a rare event (small probability level) simulation problem into a sequence of more frequent ones (Au and Beck 2001; Au and Wang 2014). Consider, for example, the slope failure probability P_f, which is defined as the probability of FS smaller than fs, i.e., $P_f=P(FS<fs)$. In the context of SS, the P_f can be expressed as (Au et al. 2010; Wang et al. 2011):

$$P_f = P(F_m) = P(F_1)\prod_{k=2}^{m} P(F_k|F_{k-1}) \tag{6}$$

where $F_k=\{FS<fs_k,\ k=1, 2, \ldots, m\}$ are a set of the intermediate failure events that are defined by a decreasing sequence of intermediate threshold values $fs_1>fs_2>\ldots>fs_m=fs$, respectively; $P(F_1)=P(FS<fs_1)$ and $P(F_k|F_{k-1})=P(FS<fs_k|FS<fs_{k-1})$, k=2, 3, …, m. During SS, fs_1, fs_2, …, fs_{m-1} are determined adaptively so that the sample estimates of $P(F_1)$ and $P(F_k|F_{k-1})$, k=2, 3, …, m−1, always correspond to a common specified value of conditional probability p_o. This is shown in Fig. 1 schematically.

As shown in Fig. 1, SS starts with direct MCS, in which N direct MCS samples are generated. The FS values of the N samples are calculated from the finite element analyses of slope stability (see "Finite element analysis of slope stability") and are ranked in a descending order. The $(1-p_o)N$-th FS value is chosen as fs_1, and hence, the sample estimate for $P(F_1)=P(FS<fs_1)$ is p_o. Then, the p_oN samples with $F_1=\{FS<fs_1\}$ are used as "seeds" for the application of Markov Chain Monte Carlo Simulation (MCMCS) to simulate $(1-p_o)N$ additional conditional samples given $F_1=\{FS<fs_1\}$, the corresponding FS values of which are calculated using SSRT during the simulation. Therefore, there are a total of N samples with $F_1=\{FS<fs_1\}$. These N FS values are ranked again in a descending order, and the $(1-p_o)N$-th FS value is chosen as fs_2, which defines the $F_2=\{FS<fs_2\}$. Note that the sample estimate for $P(F_2|F_1)=P(FS<fs_2|FS<fs_1)$ is also equal to p_o. Similarly, the procedure described above is repeated m times until the failure domain $F_m=\{FS<fs_m\}$ is achieved. Finally, a total of m+1 levels of simulations (including one direct MCS level and m levels of MCMCS) are performed, resulting in $N+m(1-p_o)N$ SS samples.

During SS, the sample space is divided into m+1 mutually exclusive and collectively exhaustive subsets Ω_k, k=0, 1, …, m, by the m intermediate threshold values fs_1, fs_2, …, fs_m, where $\Omega_o=\{FS\geq fs_1\}$, $\Omega_k=F_k-F_{k+1}=\{fs_{k+1}\leq FS<fs_k\}$ for k=1, 2, …, m−1, and $\Omega_m=F_m=\{FS<fs_m\}$. The random samples in different subsets (i.e., Ω_k, k=0, 1, …, m) carry different probability weights. For a given Ω_k, the probability weight is quantified by its occurrence probability $P(\Omega_k)$, which is taken as $p_o{}^k-p_o{}^{k+1}$ for k=0, 1, …, m−1, and $p_o{}^m$ for k=m (Au 2005; Wang and Cao 2013). Physically, the slope failure event may occur in any Ω_k, depending on the problem concerned. The plausibility of slope failure given sampling in Ω_k is quantitatively represented by the conditional failure probability $P(F|\Omega_k)$ for Ω_k, which is estimated as the fraction of the failure samples with $FS<fs$ in Ω_k. Since Ω_k, k=0, 1, …, m, are mutually exclusive and collectively exhaustive subsets and they carry different probability weights, the failure probability P_f is calculated as a summation of the plausibility (i.e., $P(F|\Omega_k)$) of slope failure given sampling in Ω_k weighted by occurrence probability (i.e., $P(\Omega_k)$) of Ω_k. This is, mathematically, expressed as the Total Probability Theorem in terms of probability concepts (Ang and Tang 2007):

$$P_f = \sum_{k=0}^{m} P(F|\Omega_k)P(\Omega_k) \tag{7}$$

Using the $N+m(1-p_o)N$ samples generated by SS and Eq. (7), the P_f is calculated accordingly. The COV_{P_f} of P_f obtained from SS relies on the correlation among the estimators of $P(F_1)$ and $P(F_k|F_{k-1})$, k=2, 3, …, m. By assuming these estimators are uncorrelated, COV_{P_f} can be expressed by (Au and Beck 2001):

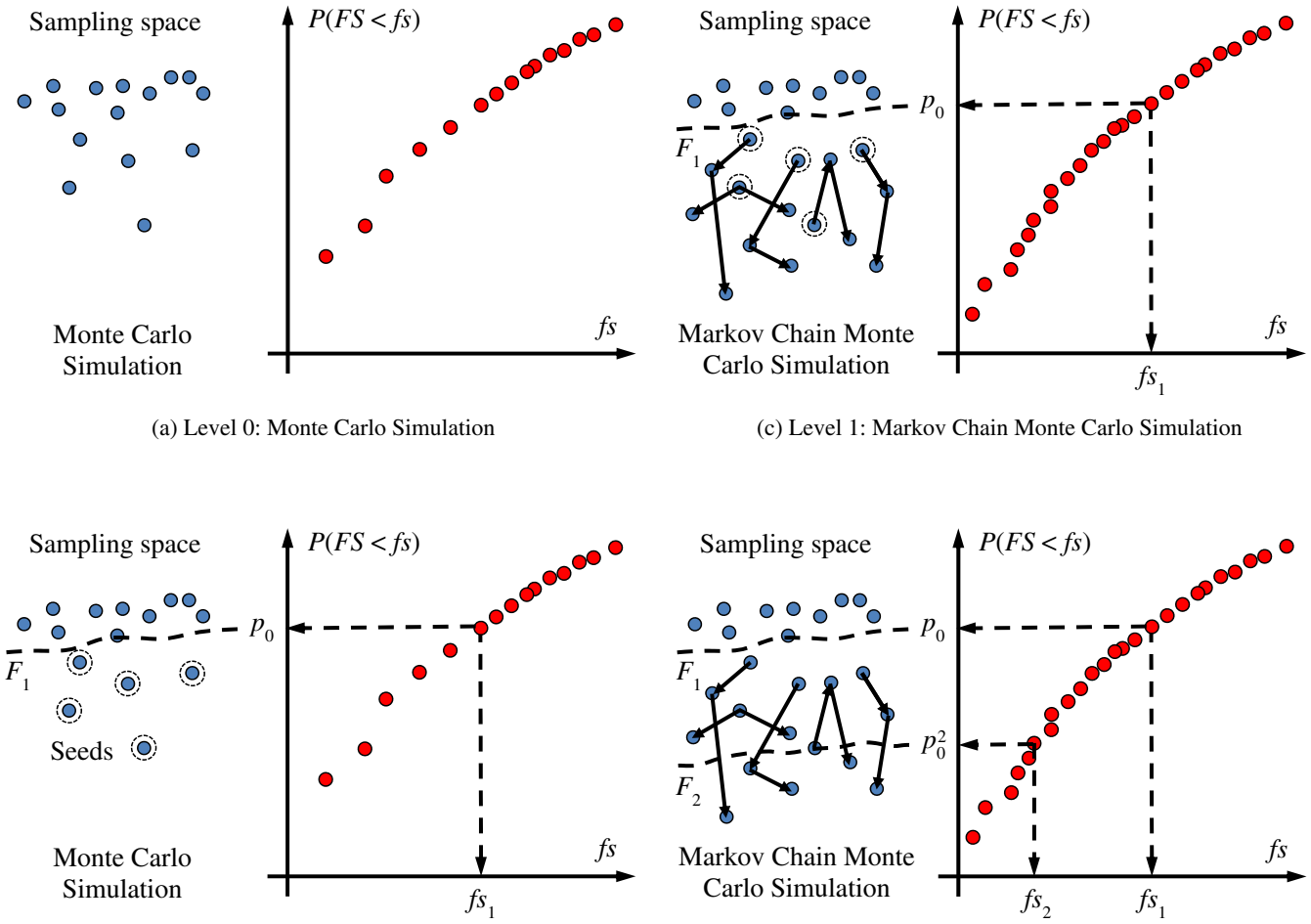

Fig. 1 Schematic diagram of Subset Simulation procedure (modified from Au et al. (2010))

$$\mathrm{COV}_{P_f} = \sqrt{\mathrm{COV}^2_{P(F_1)} + \sum_{k=2}^{m} \mathrm{COV}^2_{P\left(F_k \middle| F_{k-1}\right)}} = \sqrt{\frac{1-P(F_1)}{P(F_1)N} + \sum_{k=2}^{m} \frac{1-P(F_k|F_{k-1})}{P(F_k|F_{k-1})N}(1+\gamma_k)} \quad (8)$$

where $\mathrm{COV}_{P(F_1)} = \sqrt{\frac{1-P(F_1)}{P(F_1)N}}$ and $\mathrm{COV}_{P(F_k|F_{k-1})} = \sqrt{\frac{1-P(F_k|F_{k-1})}{P(F_k|F_{k-1})N}(1+\gamma_k)}$ are the coefficient of variation (COV) of $P(F_1)$ and $P(F_k|F_{k-1})$, respectively; and γ_k=the correlation factor, and it can be estimated from the conditional samples generated by MCMCS in the k-th simulation level. Equation (8) indicates that the variability of P_f obtained from SS is resulted from the variability of the estimators of $P(F_1)$ and $P(F_k|F_{k-1})$, which is quantitatively reflected by their respective COVs (i.e., $\mathrm{COV}_{P(F_1)}$ and $\mathrm{COV}_{P(F_k|F_{k-1})}$). Although the estimators of $P(F_1)$ and $P(F_k|F_{k-1})$, k=2, 3, …, m, are generally correlated, previous studies (e.g., Au and Beck 2001) showed that the COV_{P_f} in SS is well approximated by Eq. (8). More details and discussions on COV_{P_f} for SS are referred to Au and Beck (2001) and Au and Wang (2014).

Note that the efficient generation of conditional samples is pivotal to the success of SS, and it is made possible through the machinery of MCMCS. The MCMCS generates a sequence of samples of random variables or a random vector (e.g., uncertain parameters $\underline{\boldsymbol{X}}$=[$X_1$, X_2, …, X_{Np}] involved in slope reliability analysis) as states of Markov Chain with the probability density function (PDF) of random variables as the Markov Chain's limiting stationary distribution (e.g., Beck and Au 2002; Robert and Casella 2004). During SS, a candidate sample for next state in the Markov Chain is first generated from a proposal PDF defined using the current Markov Chain state, and it is accepted or rejected to be the next state based on the acceptance ratio and the occurrence of intermediate failure events. However, the acceptance ratio often decreases exponentially in some original MCMCS algorithms (e.g., Metropolis algorithm) as the dimension (e.g., N_p) of uncertain parameters space increases, leading to many repeated samples and reduction of computational efficiency and accuracy in high-dimensional problems (Papaioannou et al. 2014). To address this issue, a modified Metropolis algorithm (MMA) (Au and Beck 2001; Au and Wang 2014) is developed to simulate conditional samples in SS, which generates the candidate sample of a high dimensional random vector component by component. For example, using MMA to generate the candidate sample of $\underline{\boldsymbol{X}}$ contains N_p steps.

In each step, the candidate sample of X_j, j=1, 2, …, N_p, is generated. After the candidate samples of all the components are obtained, they are collectively taken as the candidate sample of $\underline{\boldsymbol{X}}$. If the $\underline{\boldsymbol{X}}$'s candidate sample belongs to the intermediate failure event concerned, it is taken as the next state of $\underline{\boldsymbol{X}}$ in the Markov Chain. Using MMA reduces the correlation among conditional samples generated by SS in high-dimensional space and, therefore, makes SS feasible in high-dimensional problems, e.g., slope reliability analysis problems that consider geotechnical spatial variability using random fields.

SS-based RFEM for risk assessment of slope failure

After the P_f is obtained, the average consequence $\overline{C}$ is still needed to evaluate the risk R of slope failure according to Eq. (5). Based on the conditional failure samples in different subsets (i.e., Ω_k, k=0, 1, …, m) that are progressively determined during SS and carry different probability weights, $\overline{C}$ is calculated as a weighted summation:

$$\overline{C} = E(C|F) = \sum_{k=0}^{m} \overline{C}_k P(\Omega_k|F) \tag{9}$$

where $E(C|F)$=the conditional expectation of the consequence given the occurrence of the slope failure; $P(\Omega_k|F)$=the probability of the failure samples falling into Ω_k; $\overline{C}_k = \sum_{i=1}^{N_{f,k}} C_{k,i}/N_{f,k}$=the average consequence of different failure modes corresponding to failure samples in Ω_k, in which $N_{f,k}$=the number of failure samples generated in Ω_k during SS and $C_{k,i}$ is the consequence of the failure mode corresponding to the i-th failure sample generated in Ω_k. Note that $C_{k,i}$ is a key input in Eq. (9) to evaluate the average consequence $\overline{C}_k$ of slope failure occurring in Ω_k. For simplicity, $C_{k,i}$ is approximately taken as the sliding mass volume for the i-th failure sample generated in Ω_k in this study, which can be determined using KMCM based on the displacements of finite element nodes, as suggested by Huang et al. (2013). Although such a simplification provides a convenient way to evaluate the "equivalent" consequence of slope failure, evaluation of the "actual" consequence of slope failure can be a complicated issue and requires more information on the site besides the sliding mass volume (e.g., Li et al. 2009; Peng et al. 2014; Vranken et al. 2014), which is worthwhile to be explored in future study. In addition, $P(\Omega_k|F)$ in Eq. (9) is calculated using the Bayes' Theorem:

$$P(\Omega_k|F) = \frac{P(F|\Omega_k)P(\Omega_k)}{P_f} \tag{10}$$

where P_f, $P(F|\Omega_k)$, and $P(\Omega_k)$ are given in Eq. (7). Using Eqs. (9) and (10) gives

$$\overline{C} = \frac{\sum_{k=0}^{m} \overline{C}_k P(F|\Omega_k)P(\Omega_k)}{P_f} \tag{11}$$

Then, substituting Eq. (11) into Eq. (5) gives

$$R = \sum_{k=0}^{m} \overline{C}_k P\left(F\middle|\Omega_k\right)P(\Omega_k) \tag{12}$$

Using Eq. (12), the risk R of slope failure is calculated using the conditional samples generated during SS. Herein, it is worthwhile to point out that although a simple and approximate way is adopted in this study to estimate the consequence of slope failure, the proposed approach is generally applicable for different methods to evaluate the slope failure consequence (e.g., $C_{k,i}$ and $\overline{C}_k$). Using a more accurate estimate of slope failure consequence in Eq. (12), of course, leads to a more accurate estimate of slope failure risk R. To gain more insights into the R estimated by SS, Eq. (12) is further written as:

$$R = \sum_{k=0}^{m} R_k P(\Omega_k) \tag{13}$$

where $R_k = P(F|\Omega_k)\overline{C}_k$ is an analogue of Eq. (5) and represents the conditional risk of slope failure in Ω_k. In the light of Eq. (13), the overall risk of slope failure can be considered as a weighed aggregation of the slope failure risk in different sampling spaces (i.e., Ω_k, k=0, 1, …, m) that are progressively determined during SS and have different occurrence probabilities. The contribution of slope failure risk (COR) in each sampling space to the overall slope failure risk is calculated as:

$$\mathrm{COR}_k = 100R_k P(\Omega_k)/R \tag{14}$$

where COR_k=contribution of the risk of slope failure occurring in Ω_k to the overall risk R in percent (%). Since the occurrence probabilities of Ω_k, k=0, 1, …, m, are different, COR_k quantifies the relative contributions of the slope failure risk at different probability levels to the overall risk R. Such insights are not provided by the original RFEM with direct MCS.

Non-intrusive implementation of SS-based RFEM in practice

Compared with the direct MCS-based RFEM, the algorithm of SS-based RFEM is somewhat more complicated, which might lead to difficulty in using the proposed approach in practice because the training of geotechnical practitioners in probability theory and statistics is often limited. To facilitate the use of the SS-based RFEM in practice, its implementation is deliberately divided into three parts in this study, including SS for uncertainty propagation, deterministic finite element analysis for evaluating FS of slope stability, and the slope failure consequence assessment using KMCM (see Fig. 2). By this means, the reliability analysis and risk assessment of slope stability can proceed as an extension of deterministic finite element analysis of slope stability in a non-intrusive manner. This allows the uncertainty propagation using SS, deterministic finite element analysis of slope stability, and slope failure consequence assessment using KMCM to be performed separately by personnel with different expertise and in a parallel fashion. SS and KMCM can be programmed as user functions or toolboxes in computer software, such as MATLAB and EXCEL (e.g., Au and Wang 2014). In this study, in-house user functions of SS and KMCM are developed in MATLAB (Mathworks Inc. 2014). These user functions can be treated as a "black box". Although a thorough understanding of reliability algorithms is always advantageous, it is not a prerequisite for engineers to use these user functions. Geotechnical practitioners only need to focus on deterministic finite element analysis of slope stability and develop a finite element model of slope stability using commercial software packages, e.g., Abaqus (Dassault Systèmes 2014). The user functions will

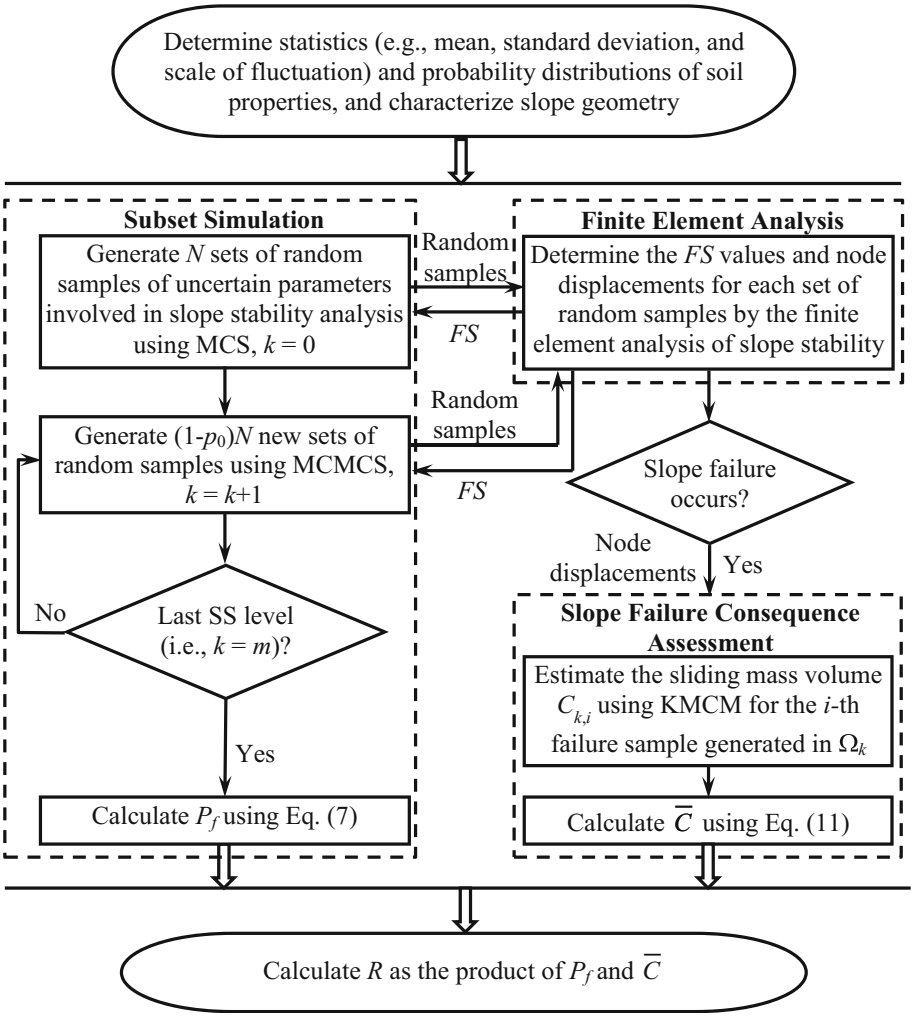

Fig. 2 Implementation procedures of SS-based RFEM for reliability analysis and risk assessment of slope stability

repeatedly invoke the finite element model of slope stability during SS and return P_f, $\overline{C}$, and R as outputs. This allows engineers to use the SS-based RFEM without being compromised by the complicated algorithms. The proposed SS-based RFEM and its implementation procedures are illustrated through a slope example in the next section.

Illustrative example

For illustration, this section applies the proposed SS-based RFEM to evaluate P_f and R of a cohesive slope example. As shown in Fig. 3, the slope has a height of 24 m and a slope angle of 36.9°, and it is comprised of two soil layers. The undrained shear strength S_{u1} and S_{u2} of the two soil layers are lognormally distributed. Their respective mean values are 80 and 120 kPa, and both of them have a COV of 0.3. In addition, the unit weights γ_1 and γ_2 of the two soil layers are taken as deterministic values, and both of them are 19 kN/m^3. To enable the finite element analysis of slope stability, the information on the Young's modulus and Poisson's ratio of the two soil layers are also needed. In the case of no available information on them, they are assumed to be 100 MPa and 0.3, respectively (Griffiths and Lane 1999). Using the information on the slope geometry and soil properties, a finite element model of the slope is created using a commercial software package Abaqus (Dassault Systèmes 2014) in this study. As shown in Fig. 3, the upper layer is discretized into 585 elements, whose horizontal and vertical side lengths are 1.33 and 1 m, respectively; and the lower layer is discretized into 711 elements with the same size. Based on the mean values of soil properties, the finite element analysis of slope stability is performed using an elastic-perfectly plastic constitutive model with a Mohr-Coulomb failure criterion in Abaqus. Then, the critical slip surface (see the dashed line in Fig. 4) is identified using KMCM based on node displacements, and its corresponding FS calculated using SSRT is 1.443.

To incorporate the effects of spatial variability of soil properties into reliability analysis and risk assessment, the inherent spatial variability of S_{u1} and S_{u2} are taken into

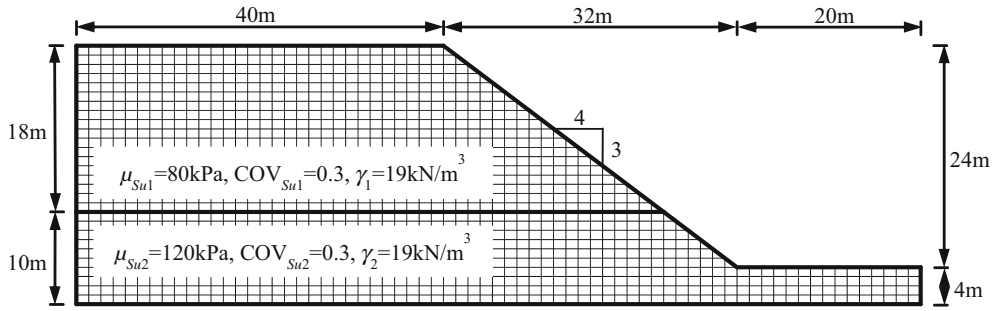

Fig. 3 An illustrative slope example

account in this example. For each parameter, the random field is simulated using Eq. (1), in which δ_h and δ_v are taken as 24 and 2.4 m, respectively. Each realization of the random field is mapped onto the finite element mesh shown in Fig. 3. Then, the finite element analysis of slope stability is performed to calculate the *FS* by SSRT and the node displacements. If the slope failure occurs (i.e., $FS<fs$), the node displacements are subsequently used to determine the critical slip surface by KMCM. Based on the critical slip surface, the slope failure consequence is estimated as the sliding mass volume. For example, Fig. 5 shows a typical realization of the random fields of S_{u1} and S_{u2} and its corresponding results of slope stability analysis obtained from the finite element analysis, including the *FS* (i.e., 0.938) calculated by SSRT, the critical slip surface identified by KMCM (see the bold solid line), and the consequence (i.e., sliding mass volume in this study) of about 882.0 m^3/m (or 882.0 m^2). Note that 2-D slope stability analysis is performed in this study. Strictly speaking, the sliding mass is an "area" but not a "volume" in this example, and it, therefore, has a unit of "m^3/m" (or "m^2" for simplicity), rather than "m^3". However, the term "sliding mass volume" is still used in this study for easy understanding and communication.

Based on the deterministic finite element model and random field model of soil parameters described above, a SS run with m=4, p_o=0.1, and N=500 is performed in this study. This leads to a total of 500+4×(1−0.1)×500=2300 random samples. Based on these 2300 random samples, P_f and R are calculated by Eqs. (7) and (12), respectively.

Results of reliability analysis and risk assessment

Table 1 summarizes the procedures of evaluation of P_f and R in this example. Among the 2300 samples from SS, 547 samples are identified as failure samples for fs=1 (i.e., FS<1). These 547 failure samples include 500 samples in simulation level 4 (i.e., all the samples in simulation level 4 fail) and 47 samples in simulation level 3, and no failure sample occurs in simulation levels 0 to 2. Using these failure samples, $P(F|\Omega_k)$ for k=0, 1, …, 4, are estimated as 0, 0, 0, 47/450, and 500/500 (see Column 3), respectively, and $\overline{C}_k$ for k=0, 1, …, 4, are calculated as 0, 0, 0, 669.11 m^2, and 648.56 m^2 (see Column 4), respectively. In addition, since p_o is taken as 0.1 in SS, $P(\Omega_k)$ for k=0, 1, …, 4, are 0.9, 0.09, 0.009, 0.0009, and 0.0001 (see Column 2), respectively. Using Eq. (7), P_f is estimated as 0.019 %, as shown in Column 6. In addition, $\overline{C}$ and R are also estimated as 658.51 m^2 (see Column 7) and 0.13 m^2 (see Column 8) by Eqs. (11) and (12), respectively. Compared with $\overline{C}$, the value of R is quite small because it is defined as the product of $\overline{C}$ and P_f in this study and P_f is relatively small (i.e., 0.019 % in this example). Since an "equivalent" quantity (i.e., the sliding mass volume) of the slope failure consequence is used in this study to estimate the slope failure risk R, the R obtained in this study is also considered as an "equivalent" quantity of the "real" risk of slope failure that accounts for the actual slope failure costs. Although the individual value of the estimated R seems meaningless, the estimated R is meaningful in a relative scale and provides a useful tool to quantify the relative contributions of slope failure risk at different probability levels to the overall risk of slope failure and to shed light on the effects of spatial variability on the slope, as discussed later in this paper.

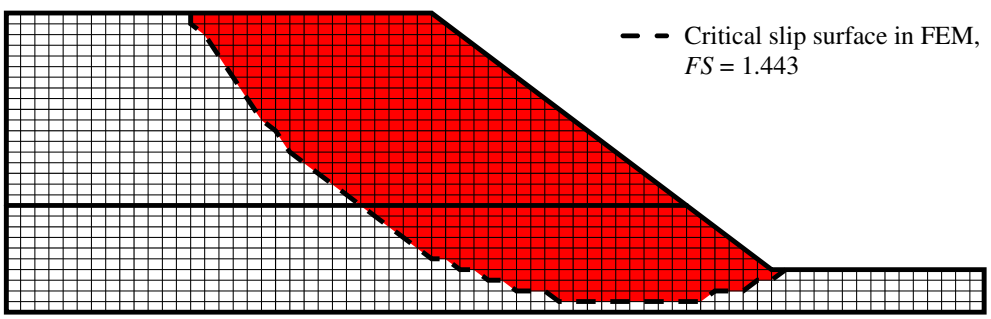

Fig. 4 Results of deterministic slope stability analysis

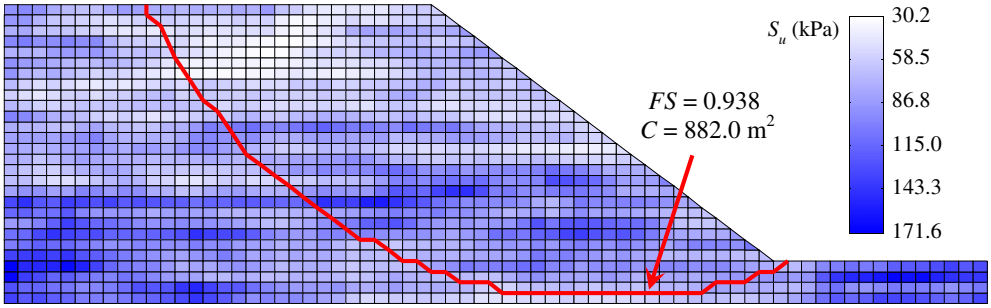

Fig. 5 A typical realization of random fields and its corresponding results of slope stability analysis

As indicated by Eq. (13), the risk of slope failure is de-aggregated into different sampling spaces Ω_k, k=0, 1, …, 4. The relative contributions of slope failure risk occurring in these sampling spaces are calculated using Eq. (14), and they are 0, 0, 0, 49, and 51 % (see Column 5), respectively. The overall risk of slope failure is attributed to the slope failure occurring in Ω_3 and Ω_4 in this example. To enable a desired accuracy of the estimated R, a large number of failure samples shall be generated in Ω_4. This can be achieved through SS with relative ease. As shown in Table 1, all the 500 samples generated in Ω_4 by SS are failure samples. On the other hand, if using direct MCS to generate such a number of samples in Ω_4, a total of 500/0.0001=5,000,000 samples are required on average, because $P(\Omega_4)$=0.0001. Compared with direct MCS, the proposed SS-based RFEM not only provides more insights (e.g., contributions of slope failure risk in different sampling spaces or at different probability levels) into the overall risk R, but also improves significantly the computational efficiency of generating the samples of interest (e.g., samples in Ω_4) for slope risk assessment. This is of particular importance for RFEM, as further discussed in the next subsection.

Validation of reliability analysis and risk assessment results

To validate the reliability analysis and risk assessment results obtained from the SS-based RFEM, a direct MCS run with 60,000 samples is performed to calculate the P_f and R of the slope example. Figure 6 shows the variation of the failure probability P_f=$P(FS<fs)$ as a function of fs (i.e., the cumulative distribution function of FS) obtained from direct MCS and SS by a dashed line and a solid line, respectively. The solid line generally plots closely to the dashed line. For fs=1, the P_f estimated from direct MCS is 0.018 %, which agrees well with the value (i.e., 0.019 %) of P_f obtained from SS. Such observations indicate that the P_f is calculated properly using the SS-based RFEM proposed in this study. Note that only 2300 random samples are generated in the SS-based RFEM, and hence a total of 2300 finite element analyses of slope stability are performed, which are much less than the number (i.e., 60,000) of finite element analyses of slope stability required in the original RFEM with direct MCS.

Table 2 summarizes the reliability analysis results obtained from direct MCS and SS. It takes 20.8 days (d) to finish 60,000 finite element analyses of slope stability in direct MCS on a desktop computer with 8 GB RAM and one Intel Core i7 CPU clocked at 3.4 GHz. On the other hand, 2300 finite element analyses of slope stability in SS are finished within a day, specifically in 0.8 d, on the same computer. In addition, the COV_{P_f} values are also calculated from a single direct MCS run with 60,000 samples using Eq. (3) and a single SS run with 2300 samples using Eq. (8), and they are about 0.3 and 0.37 (see Column 6 in Table 2), respectively. To validate the COV_{P_f} estimated from Eq. (8) for SS, 20 independent SS runs are performed, which give 20 P_f values. Using these 20 P_f values, the COV_{P_f} is estimated as 0.38, which is almost identical to the value (i.e., 0.37) given by Eq. (8) in this example. To enable a fair comparison of the computational efficiency and eliminate effects of sample size on COV_{P_f}, the values of unit COV, defined as $\mathrm{COV}_{P_f} \times \sqrt{N_T}$ (Au and Beck 2003), are calculated for direct MCS and SS. As shown in Table 2, the unit COV (i.e., 73.5) in direct MCS-based RFEM is about four times larger than that (i.e., 17.7) in SS-based RFEM. The above observations demonstrate that integrating SS with RFEM improves, significantly, the computational efficiency at small probability levels and reduces the computational time. This enhances the applications of RFEM in

Table 1 Results of reliability analysis and risk assessment in the slope example

Simulation level k	$P(\Omega_k)$	$P(F\|\Omega_k)$	$\overline{C}_k$ (m^2)	COR_k (%)	P_f (%)	$\overline{C}$ (m^2)	R (m^2)
0	0.9	0	0	0	0.019	658.51	0.13
1	0.09	0	0	0			
2	0.009	0	0	0			
3	0.0009	47/450	669.11	49			
4	0.0001	500/500	648.56	51			

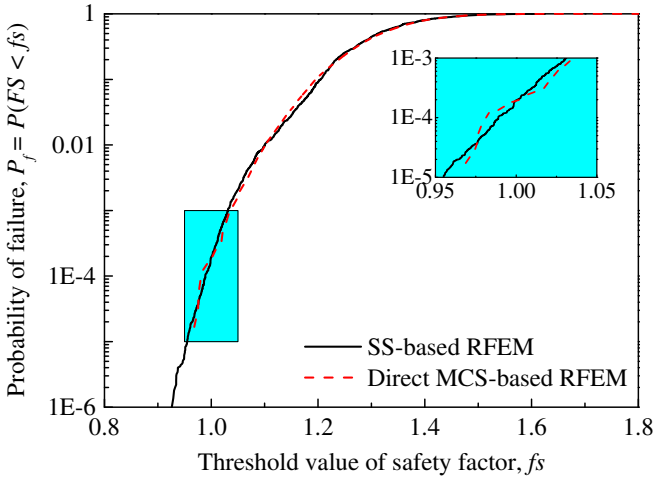

Fig. 6 Cumulative distribution function of the performance function of slope stability

the slope reliability analysis, particularly at small probability levels (e.g., P_f<0.001).

Figure 7 shows the estimated $\overline{C}$ for different *fs* values (i.e., 1.0, 1.05, …, 1.3) obtained from RFEM with SS and direct MCS by the lines with squares and circles, respectively. The line with squares plots closely to the line with circles. The $\overline{C}$ values estimated from the SS-based RFEM are in good agreement with those obtained from the original RFEM with direct MCS. In addition, it is also noted that the estimated $\overline{C}$ almost remains unchanged around 670 m² as *fs* varies in this example. Figure 8 shows the variation of *R* as a function of *fs* obtained from RFEM with SS and direct MCS by the lines with squares and circles, respectively. The *R* values estimated from the SS-based RFEM agree well with those obtained from the original RFEM with direct MCS. This further validates the risk assessment results obtained from the SS-based RFEM.

As shown in Fig. 8, *R* increases significantly as *fs* increases. Note that the desired safety level of the slope increases with the increase of *fs*. As expected, for a given slope problem, *R* increases as the desired safety level increases. Such an increase in *R* is mainly attributed to the increase in P_f (see Fig. 6), since $\overline{C}$ remains almost unchanged in this example (see Fig. 7). The proposed approach properly depicts the slope failure risk at different safety levels using a single SS run.

Effects of vertical spatial variability on the slope failure risk

With the aid of improved computational efficiency offered by the SS-based RFEM, this subsection performs a sensitivity study to explore effects of spatial variability with the depth on the slope failure risk. Figure 9 shows the *R* estimated from the SS-based RFEM for different δ_v values (i.e., 2.4, 6, 12, and 24 m). As δ_v increases from 2.4 to 24 m (i.e., the vertical spatial variability becomes weaker), the estimated *R* increases by about two orders of magnitude in this example. Therefore, the vertical spatial variability affects *R* significantly. To gain more insights into such effects on *R*, effects of vertical spatial variability on P_f and $\overline{C}$ are further investigated, respectively. Figure 10 shows the variations of P_f and $\overline{C}$ as a function of δ_v by the lines with squares and circles, respectively. The estimated P_f increases by about two orders of magnitude in this example when δ_v increases from 2.4 to 24 m. The δ_v affects P_f significantly. On the other hand, the estimated $\overline{C}$ only decreases slightly as δ_v increases (see the line with circles in Fig. 10). The effect of vertical spatial variability on $\overline{C}$ is minimal. Since *R* is defined as the product of P_f and $\overline{C}$, it can be reasoned that, as δ_v increases, the increase in *R* is mainly attributed to the increase in P_f in this example. The effects of vertical spatial variability are properly incorporated into risk assessment of slope failure using the proposed SS-based RFEM.

Summary and conclusions

This paper developed an efficient random finite element method (RFEM) for reliability analysis and risk assessment of slope stability. The proposed approach integrates RFEM with an advanced MCS method called "Subset Simulation (SS)" to evaluate the slope failure probability (P_f) and risk (*R*) in spatially variable soils. The proposed SS-based RFEM expresses the overall risk of slope failure as a weighed aggregation of slope failure risk at different probability levels that are progressively determined during SS. It quantifies the relative contributions of the slope failure risk at different probability levels to the overall risk *R* of slope failure. Such insights are not available in direct MCS-based RFEM. In addition, SS is deliberately decoupled from the deterministic finite element analysis of slope stability in the proposed approach, so that the reliability analysis and risk assessment of slope stability using RFEM can proceed as an extension of deterministic finite element analysis of slope stability in a non-intrusive manner. This effectively removes the hurdle of reliability computational algorithms and allows geotechnical practitioners to focus on the deterministic slope stability analysis that they are familiar with.

Table 2 Comparison of results obtained from direct MCS-based RFEM and SS-based RFEM

Method	Number of samples	Number of failure samples	Time (d)[a]	P_f (%)	COV_{P_f}	Unit COV[c]
Direct MCS-based RFEM	60,000	11	20.8	0.018	0.30	73.5
SS-based RFEM	2300	547 (536[b])	0.8	0.019 (0.017[b])	0.37 (0.38[b])	17.7 (18.2[b])

[a] Performed on a desktop computer with 8 GB RAM and one Intel Core i7 CPU clocked at 3.4 GHz

[b] The results based on 20 independent SS runs

[c] Unit COV=$COV_{P_f} \times \sqrt{N_T}$

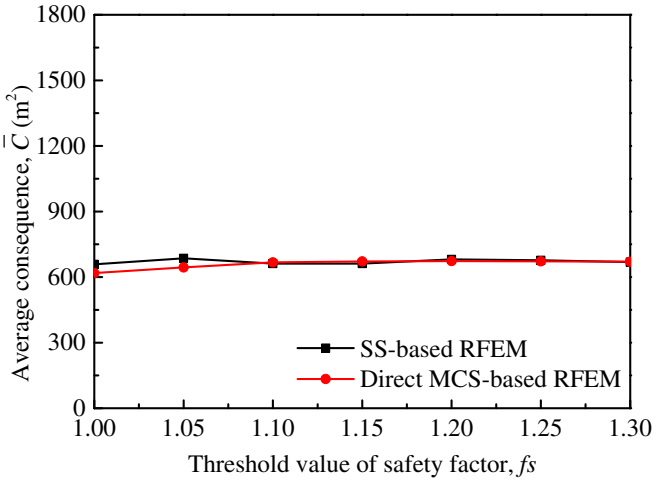

Fig. 7 Average consequence at different safety levels

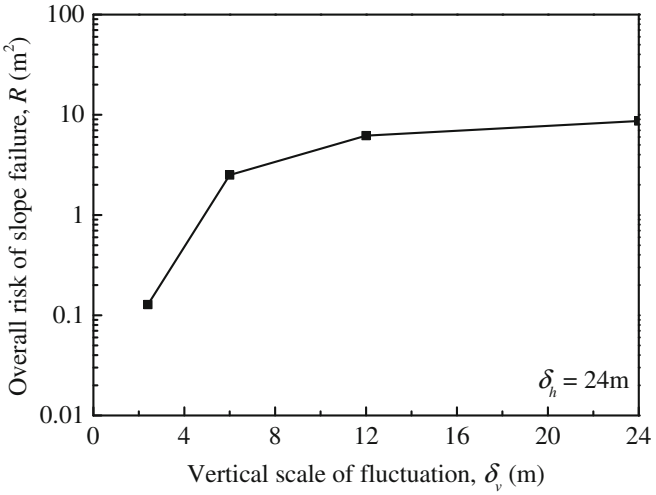

Fig. 9 Effects of vertical spatial variability on slope failure risk

Equations were derived for evaluating P_f and R using the random samples generated by SS. These equations were illustrated using a soil slope example. The results obtained from the SS-based RFEM are validated against those obtained using the direct MCS-based RFEM. It was shown that the P_f and R at different safety levels (i.e., different fs values) are calculated properly using the proposed approach. Compared with the direct MCS-based RFEM, integrating SS with RFEM improves, significantly, the computational efficiency of generating failure samples for evaluating P_f and R. This enhances the applications of RFEM in the reliability analysis and risk assessment of slope stability, particularly at small probability levels (e.g., P_f<0.001). With the aid of improved computational efficiency, a sensitivity study was performed to explore the effects of vertical spatial variability on the slope failure risk. It was found that the vertical spatial variability affects significantly the slope failure risk.

In the end, it is also worthwhile to point out that although the computational effort is significantly reduced by SS-based RFEM in terms of time and number of finite element analyses of slope stability (from 20.8 to 0.8 d and from 60,000 to 2300 in the slope example), thousands of finite element analyses are still required at extremely small probability levels (e.g., P_f<10^{-4}~10^{-5}). It might take a few days to finish the calculation on a commonly used desktop computer (e.g., the one used in this study) at such small probability levels. More importantly, the computational time generally increases as the finite element model becomes more sophisticated. This possibly occurs when a finer finite element mesh and/or advanced soil constitutive models are applied in the finite element analysis of slope stability, the slope geometry increases, or a three-dimensional slope problem is concerned. In such a case, evaluating slope failure probability and risk by RFEM with the consideration of spatial variability at small probability levels is still a computationally intensive problem and is not a trivial task in slope engineering practice. More efforts on this aspect are still needed in future study.

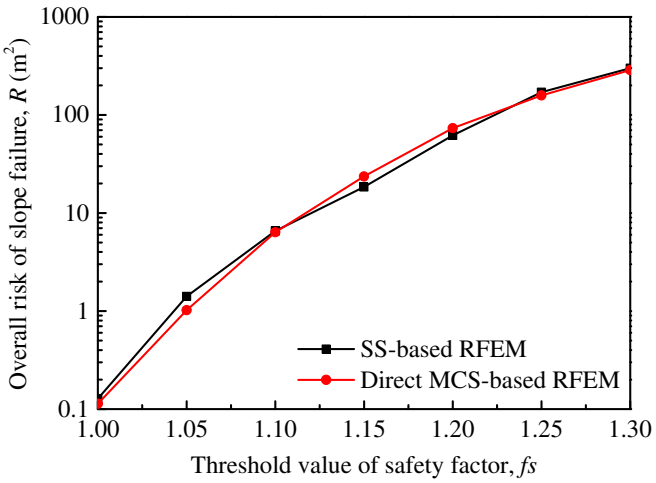

Fig. 8 Overall risk of slope failure at different safety levels

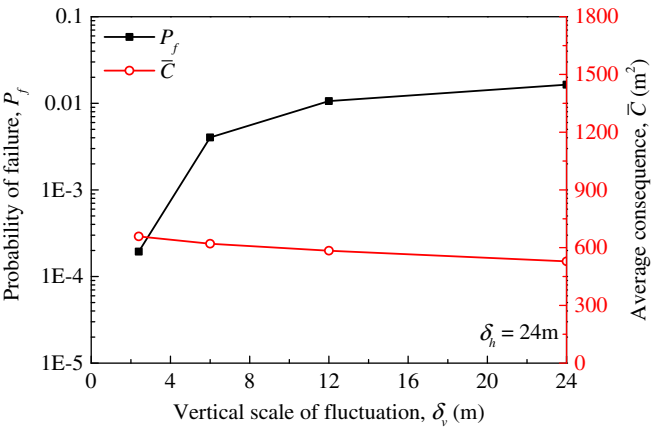

Fig. 10 Effects of vertical spatial variability on the probability of slope failure and the average consequence

Acknowledgments

This work was supported by the National Science Fund for Distinguished Young Scholars (Project No. 51225903), the National Basic Research Program of China (973 Program) (Project No. 2011CB013506), the National Natural Science Foundation of China (Project No. 51329901, 51409196), the Natural Science Foundation of Hubei Province of China (Project No. 2014CFA001), an open fund from State Key Laboratory Hydraulics and Mountain River Engineering, Sichuan University (Project No. SKHL1318), and the Fundamental Research Funds for the Central Universities (Project No. 2042014kf0001). The financial support is gratefully acknowledged.

References

Ang AH-S, Tang WH (2007) Probability concepts in engineering: emphasis on applications to civil and environmental engineering, 2nd edn. John Wiley & Sons, Hoboken

Au SK (2005) Reliability-based design sensitivity by efficient simulation. Comput Struct 83(14):1048–1061

Au SK, Beck JL (2001) Estimation of small failure probabilities in high dimensions by subset simulation. Probabilistic Eng Mechanics 16(4):263–277

Au SK, Beck JL (2003) Important sampling in high dimensions. Struct Saf 25(2):139–163

Au SK, Wang Y (2014) Engineering risk assessment with subset simulation. John Wiley & Sons, Singapore

Au SK, Cao ZJ, Wang Y (2010) Implementing advanced Monte Carlo simulation under spreadsheet environment. Struct Saf 32(5):281–292

Beck JL, Au SK (2002) Bayesian updating of structural models and reliability using Markov chain Monte Carlo simulation. J Eng Mech 128(4):380–391

Cao Z, Wang Y (2014) Bayesian model comparison and selection of spatial correlation functions for soil parameters. Struct Saf 49:10–17

Ching J, Phoon KK, Hu YG (2009) Efficient evaluation of reliability for slopes with circular slip surfaces using importance sampling. J Geotech Geoenviron 135(6):768–777

Cho SE (2010) Probabilistic assessment of slope stability that considers the spatial variability of soil properties. J Geotech Geoenviron 136(7):975–984

Cho SE (2013) First-order reliability analysis of slope considering multiple failure modes. Eng Geol 154:98–105

Chowdhury RN, Xu DW (1995) Geotechnical system reliability of slopes. Reliability Eng System Safety 47(3):141–151

Christian JT, Ladd CC, Baecher GB (1994) Reliability applied to slope stability analysis. J Geotech Eng 120(12):2180–2207

Dassault Systèmes (2014) Abaqus Unified FEA. http://www.3ds.com/products-services/simulia/portfolio/abaqus/latest-release/

Duncan JM, Wright SG (2005) Soil strength and slope stability. John Wiley & Sons, Hoboken

El-Ramly H, Morgenstern NR, Cruden DM (2002) Probabilistic slope stability analysis for practice. Can Geotech J 39(3):665–683

Fenton GA, Griffiths DV (2008) Risk assessment in geotechnical engineering. John Wiley & Sons, Hoboken

Fenton GA, Vanmarcke EH (1990) Simulation of random fields via local average subdivision. J Eng Mech 116(8):1733–1749

Griffiths DV, Fenton GA (2004) Probabilistic slope stability analysis by finite elements. J Geotech Geoenviron 130(5):507–518

Griffiths DV, Lane PA (1999) Slope stability analysis by finite elements. Geotechnique 49(3):387–403

Griffiths DV, Huang J, Fenton GA (2009) Influence of spatial variability on slope reliability using 2-D random fields. J Geotech Geoenviron 135(10):1367–1378

Hassan AM, Wolff TF (1999) Search algorithm for minimum reliability index of earth slopes. J Geotech Geoenviron 125(4):301–308

Huang J, Griffiths DV, Fenton GA (2010) System reliability of slopes by RFEM. Soils Found 50(3):343–353

Huang J, Lyamin AV, Griffiths DV, Krabbenhoft K, Sloan SW (2013) Quantitative risk assessment of landslide by limit analysis and random fields. Comput Geotech 53:60–67

Ji J, Low BK (2012) Stratified response surfaces for system probabilistic evaluation of slopes. J Geotech Geoenviron 138(11):1398–1406

Jiang SH, Li DQ, Zhang LM, Zhou CB (2014) Slope reliability analysis considering spatially variable shear strength parameters using a non-intrusive stochastic finite element method. Eng Geol 168:120–128

Jiang SH, Li DQ, Cao ZJ, Zhou CB, Phoon KK (2015) Efficient system reliability analysis of slope stability in spatially variable soils using Monte Carlo simulation. J Geotech Geoenviron Eng ASCE 141(2):04014096

Le TMH (2014) Reliability of heterogeneous slopes with cross-correlated shear strength parameters. Georisk: Assessment Manag Risk for Engineered Systems Geohazards 8(4):250–257

Li DQ, Zhang LM, Zhou CB, Lu WB (2009) Risk based stabilization planning for soil cut slopes. Nat Hazards Earth Syst Sci 9(4):1365–1379

Li DQ, Chen YF, Lu WB, Zhou CB (2011) Stochastic response surface method for reliability analysis of rock slopes involving correlated non-normal variables. Comput Geotech 38(1):58–68

Li L, Wang Y, Cao Z, Chu X (2013) Risk de-aggregation and system reliability analysis of slope stability using representative slip surfaces. Comput Geotech 53:95–105

Li DQ, Qi XH, Phoon KK, Zhang LM, Zhou CB (2014) Effect of spatially variable shear strength parameters with linearly increasing mean trend on reliability of infinite slopes. Struct Saf 49:45–55

Low BK, Gilbert RB, Wright SG (1998) Slope reliability analysis using generalized method of slices. J Geotech Geoenviron 124(4):350–362

Mathworks Inc. (2014) MATLAB - The Language of Technical Computing. http://www.mathworks.com/products/matlab/

Matsui T, San K-C (1992) Finite element slope stability analysis by shear strength reduction technique. Soils Found 32(1):59–70

Papaioannou I, Betz W, Zwirglmaier K, Straub D (2014) MCMC algorithms for subset simulation. Manuscript. Engineering Risk Analysis Group, TU München

Peng L, Xu S, Hou J, Peng J (2014) Quantitative risk analysis for landslides: the case of the Three Gorges area, China. Landslides 1–18

Phoon KK, Huang SP, Quek ST (2002) Implementation of Karhunen–Loeve expansion for simulation using a wavelet-Galerkin scheme. Probabilistic Eng Mechanics 17(3):293–303

Robert CP, Casella G (2004) Monte Carlo statistical methods. Springer, New York

Tang XS, Li DQ, Zhou CB, Phoon KK (2015) Copula-based approaches for evaluating slope reliability under incomplete probability information. Struct Saf 52:90–99

Vanmarcke EH (2010) Random fields: analysis and synthesis (revised and expanded, newth edn). World Scientific Publishing Co. Pte. Ltd., Singapore

Vranken L, Vantilt G, Van Den Eeckhaut M, Vandekerckhove L, Poesen J (2014) Landslide risk assessment in a densely populated hilly area. Landslides 1–12

Wang Y, Cao Z (2013) Expanded reliability-based design of piles in spatially variable soil using efficient Monte Carlo simulations. Soils Found 53(6):820–834

Wang Y, Cao Z, Au SK (2011) Practical reliability analysis of slope stability by advanced Monte Carlo simulations in a spreadsheet. Can Geotech J 48(1):162–172

Zhang J, Zhang LM, Tang WH (2011) New methods for system reliability analysis of soil slopes. Can Geotech J 48(7):1138–1148

D.-Q. Li · T. Xiao · Z.-J. Cao (✉) · C.-B. Zhou
State Key Laboratory of Water Resources and Hydropower Engineering Science,
Key Laboratory of Rock Mechanics in Hydraulic Structural Engineering
(Ministry of Education), Wuhan University, 8 Donghu South Road, Wuhan, 430072,
People's Republic of China
e-mail: zijuncao@whu.edu.cn

L.-M. Zhang
Department of Civil and Environmental Engineering, The Hong Kong University
of Science and Technology, Clear Water Bay, Kowloon, Hong Kong

Z.-J. Cao
State Key Laboratory of Hydraulics and Mountain River Engineering
Sichuan University, Chengdu, 610065, People's Republic of China